

REPORT DOCUMENTATION PAGE

Form Approved
OMB No. 0704-0188

Public reporting burden for this collection of information is estimated to average 1 hour per response, including the time for reviewing instructions, searching existing data sources, gathering and maintaining the data needed, and completing and reviewing the collection of information. Send comments regarding this burden estimate or any other aspect of this collection of information, including suggestions for reducing this burden, to Washington Headquarters Services, Directorate for Information Operations and Reports, 1215 Jefferson Davis Highway, Suite 1204, Arlington, VA 22202-4302, and to the Office of Management and Budget, Paperwork Reduction Project (0704-0100), Washington, DC 20503.

19970207 014

DTIC QUALITY INSPECTED 4

14. SUBJECT TERMS			15. NUMBER OF PAGES
			16. PRICE CODE
17. SECURITY CLASSIFICATION OF REPORT	18. SECURITY CLASSIFICATION OF THIS PAGE	19. SECURITY CLASSIFICATION OF ABSTRACT	20. LIMITATION OF ABSTRACT
UNCLASSIFIED	UNCLASSIFIED	UNCLASSIFIED	

**Computer Simulations Of Radiation Generation From
Relativistic Electron Beams**

F49620-93-1-0366

AASERT FINAL TECHNICAL REPORT

TO

AIR FORCE OFFICE OF SCIENTIFIC RESEARCH

Graduate Student : Mark Hogan

Principal Investigator : Anthony T. Lin

Department of Physics
University of California, Los Angeles
Los Angeles, CA 90024-1547

June 1, 1993, to November 30, 1996

TABLE OF CONTENTS

	Page
I. Introduction	3
II. Summary of Work Accomplished	3
A. Algorithm for Isolating Transverse Current	3
B. Using B-Spline To Solve Poisson's Equation	14
C. Space Charge Effects in Gyro Backward Wave Oscillators	

I. Introduction

This is the AASERT Final Technical Report on work performed under the support of the Air Force Office of Scientific Research under Grant F49620-93-1-0366 for the period June 1, 1993 to November 30, 1996. The objective of this work was to train graduate student and teach him how to use particle-in-cell code to simulate the process of radiation generation from relativistic electron beams. At the same time, we have developed a new version of particle-in-cell code.

2. Summary of Work Accomplished

In this work, we have developed a new version of particle-in-cell code which is capable of separately following the evolution of electromagnetic and electrostatic fields. The new code was utilized to investigate the space charge effects in gyro backward wave oscillators.

The electron-wave interaction in microwave devices is a highly nonlinear phenomenon and requires computer simulations to follow its evolution. The electron convection current calculated in simulation often contains both the electromagnetic and electrostatic components. This total current is usually used as the source for exciting the electric and magnetic fields in electrodynamic structures. In this approach, it is important to make sure that the equation of continuity is satisfied at all time. In MAGIC¹, this is accomplished by correcting the electric field at every time step to insure that Poisson's equation is satisfied. Most of the other approaches employed to simulate microwave devices use medium electron beam current and assume fixed transverse field profiles determined from the boundary conditions of the structure. The electrostatic field evaluated from the Poisson equation is often added to the fields generated by the total current. In doing so, the dominant mode of space charge fields is doubly counted². In order to be able to correctly investigate the effects of space charge field on the performance of microwaves devices, we have developed a new version of particle-in-cell code which is capable of isolating the transverse current from the total current. The new code is used to simulate gyro backward wave oscillators and the result is presented in the report. In the future, the same algorithm will be applied to simulate plasma-filled backward wave oscillators and helix traveling wave amplifiers.

A. Algorithm for Isolating Transverse Current

By using the Coulomb gauge³, the current density (or electric field) can be written as the sum of two terms,

$$\vec{J} = \vec{J}_\ell + \vec{J}_t \quad (1)$$

\vec{J}_ℓ is called the longitudinal (irrotational, $\nabla \times \vec{J}_\ell = 0$) current and is the driving source for electrostatic fields, while \vec{J}_t is called the transverse (solenoidal, $\nabla \cdot \vec{J}_t = 0$) current and is the driving source for electromagnetic fields. The magnetic field, of course, only has transverse components. Starting from the vector identity,

$$\nabla \times (\nabla \times \vec{J}) = \nabla (\nabla \cdot \vec{J}) - \nabla^2 \vec{J}, \quad (2)$$

the transverse current can be determined from the total current

$$\nabla^2 (\vec{J}_t) = -\nabla \times \nabla \times \vec{J} = \nabla^2 \vec{J} - \nabla \cdot (\nabla \times \vec{J}) \quad (3)$$

The solution of Eq. (3) in integral form is³

$$\vec{J}_t = \frac{1}{4\pi} \nabla \times \nabla \times \int \frac{\vec{J}}{(\vec{x} - \vec{x}')} d^3x' \quad (4)$$

This form of solution is difficult to solve numerically. In the differential formulation, Eq. (3) can be easily solved if the field quantity is expanded into a series of complete orthogonal functions. For example, sets of such functions are the Fourier series and the Bessel functions which are the solutions for cylindrical waveguides. Consider an infinite and periodic system. In this case it is convenient to solve Maxwell's equations in the Fourier space⁴ and the

splitting of the current into transverse and longitudinal components can be easily done. From Eq. (3), the transverse current can be written as

$$\vec{J}_t = \vec{J} - \frac{\vec{k}(\vec{k} \cdot \vec{J})}{k^2} \quad (5)$$

where \vec{k} is the wavevector. Based on this approach, for the last two decades, we have unravelled numerous interesting nonlinear phenomena in plasma physics.

In microwave devices, a cylindrical waveguide (r, θ, z) is often provided to confine the electromagnetic wave propagation along the axial direction. A combination of Bessel's functions can always be found to satisfy the proper boundary conditions and Maxwell's equations. We shall first develop an algorithm under the assumption of axial symmetry. In this situation, the electromagnetic field profiles can be expressed in terms of the TE_{0n} and TM_{0n} modes. Since the electric field in the TE_{0n} mode⁵ is only along the θ direction and is independent of the θ coordinate ($\nabla \cdot \vec{E} = 0$), it contains only the electromagnetic component. For the TM_{0n} mode, the electric fields are along the z and r directions. To obtain the transverse current from the total current, Eq. (3) can be used. Take the spatial variation of the electron beam current to conform the electric field variation

$$\vec{J} = \left[\hat{z} J_z J_0 \left(p_{0n} \frac{r}{a} \right) + \hat{r} J_r J_1 \left(p_{0n} \frac{r}{a} \right) \right] e^{ik_z z} \quad (6)$$

where a is the waveguide radius and p_{0n} is the zero of the Bessel functions J_0 . The first term of the right-hand side of Eq. (3) becomes

$$\begin{aligned} \nabla (\nabla \cdot \vec{J}) &= \left[\hat{z} \left(-k_z^2 J_z + \frac{ik_z p_{0n}}{a} J_r \right) J_0 \left(\frac{p_{0n} r}{a} \right) \right. \\ &\quad \left. + \hat{r} \left(-ik_z \frac{p_{0n}}{a} J_z - \frac{p_{0n}^2}{a^2} J_r \right) J_1 \left(\frac{p_{0n} r}{a} \right) \right] e^{ik_z z}. \end{aligned} \quad (7)$$

The transverse current can be written as

$$\begin{aligned}
 J_{tz} &= -\left(\frac{p_{0n}^2}{a^2} J_z + \frac{ik_z p_{0n}}{a} J_r\right) J_0(p_{0n} \frac{r}{a}) e^{ik_z z} / \left(\frac{p_{0n}^2}{a^2} + k_z^2\right), \\
 J_{tr} &= -\left(k_z^2 J_r - \frac{ik_z p_{0n}}{a} J_z\right) J_1(p_{0n} \frac{r}{a}) e^{ik_z z} / \left(\frac{p_{0n}^2}{a^2} + k_z^2\right).
 \end{aligned} \tag{8}$$

Notice that Eq.(8) is divergence free. These currents are retained as the source to advance the electromagnetic fields through Maxwell's equation.

$$\begin{aligned}
 \frac{\partial \vec{E}_t}{\partial t} &= c \nabla \times \vec{B} - 4\pi \vec{J}_t \\
 \frac{\partial \vec{B}}{\partial t} &= -c \nabla \times \vec{E}_t
 \end{aligned} \tag{9}$$

In the next section, the electrostatic field will be evaluated from Poisson's equation.

B. Using B-Spline to Solve Poisson's Equation

For electromagnetic wave problems, the field in the exterior of the electron beam takes the form of a wave moving outwards if there is no structure to confine the wave propagation. In a cylindrical waveguide, the transverse mode is a global mode and one mode is often sufficient to represent the electron-electromagnetic wave interaction. For electrostatic problems the fields outside the beam location decay exponentially, with no oscillation spatially and no wave propagation. To simulate this localized field, a great many transverse modes are needed along the radial direction. The scheme of using finite-differencing or B-spline may be a better approach to evaluate the electrostatic field. Here, we shall describe the B-spline scheme for solving the Poisson equation.

The two-dimensional Poisson equation in cylindrical coordinates (r, z) is

$$\frac{\partial^2 \Phi}{\partial r^2} + \frac{1}{r} \frac{\partial \Phi}{\partial r} + \frac{\partial^2 \Phi}{\partial z^2} = -4\pi\rho. \tag{10}$$

The boundary conditions are $\Phi(r,0) = \Phi(r,L) = \Phi(a,z) = 0$. Expand the functions Φ and ρ along the z-direction in terms of sine functions

$$\begin{aligned}\Phi &= \sum_{k=1}^{N_z} \Phi_k(r) \sin \frac{k\pi}{L} z, \\ \rho &= \sum_{k=1}^{N_z} \rho_k(r) \sin \frac{k\pi}{L} z,\end{aligned}\tag{11}$$

where N_z is the number of grid points in the z-direction. Substituting Eq.(11) into Eq.(10) yields

$$\Phi_k'' + \frac{1}{r} \Phi_k' - \left(\frac{k\pi}{L}\right)^2 \Phi_k = -4\pi \rho_k, \tag{12}$$

where prime denotes taking derivative with respect to the r coordinate.

The collocation method with B-splines⁶ is used to numerically solve Eq.(12). Let $\{r_i\}_{1}^{N_r}$ be the radial grid points (knots), $0 = r_1 < \dots < r_{N_r} = a$. The solution of Eq.(12) can be approximated by a spline S of fourth order on the grid $\{r_i\}$. A spline can be expressed in the following form

$$S(r) = \sum_{i=1}^n a_i B_i(r), \tag{13}$$

where $B_i(r)$ are so called B-splines which are basic functions of the space of all cubic splines on the grid $\{r_i\}$. $n = N_r + 2$ is the dimension of this space⁷. Substituting $S(r)$ for $\Phi(r)$ in Eq.(12) we obtain

$$\sum_{i=1}^n a_i^{(k)} \left[B_i'' + \frac{1}{r} B_i' - \left(\frac{k\pi}{a}\right)^2 B_i \right] = -4\pi \rho_k \tag{14}$$

Since the values of ρ_k are known at the grid point r_j , we will evaluate Eq.(14) at these points to determine the coefficients $a_i^{(k)}$.

$$\sum_{i=1}^n a_i^{(k)} [B_i''(r_j) + \frac{1}{r_j} B_i'(r_j) - \left(\frac{k\pi}{a}\right)^2 B_i(r_j)] = -4\pi\rho_k(r_j), \\ j = 2, 3, \dots, N_r \quad (15)$$

Because the term $\frac{\Phi'}{r}$ in Eq.(10) is singular at $r = 0$, we must treat it carefully. The property of axis-symmetry implies $E_r = -\Phi' = 0$ at $r = 0$. The L'Hospital rule can be used to evaluate this singular term

$$\lim_{r \rightarrow 0} \frac{1}{r} \Phi' = \lim_{r \rightarrow 0} \Phi'' = \Phi''(0). \quad (16)$$

Using Eq.(16), Eq.(14) at $r = 0$ becomes

$$\sum_{i=1}^n a_i^{(k)} [2 B_i''(0) - \left(\frac{k\pi}{a}\right)^2 B_i(0)] = -4\pi\rho_k(0). \quad (17)$$

Besides Eq.(15) and (17), we have two additional boundary conditions $\Phi'(0) = 0$ and $\Phi_k(a) = 0$. In terms of B-splines, these become $\sum_{i=1}^n a_i^{(k)} B_i'(0) = 0$ and $\sum_{i=1}^n a_i^{(k)} B_i(a) = 0$. Now we have altogether $N_r + 2$ equations for $N_r + 2$ unknown coefficients $a_i^{(k)}$ and the resulting equation can be written in the form of tridiagonal matrix. After $a_i^{(k)}$ have been evaluated, the electrostatic field can be determined from $\vec{E}_s = -\nabla \times \Phi$.

C. Space Charge Effects in Gyro Backward Wave Oscillators

The new version of particle-in-cell code described in the previous sections was used to simulate the performance of gyro backward wave oscillators. The parameters (table I) used in simulations is also roughly the parameters employed in a recent experiment carried out at Phillip's Laboratory. The experimental results show very low efficiency (less than 0.1%) when the TE₀₁ mode was used.

Table I: Parameters of the gyro backward wave oscillator

Waveguide radius (r_w)	4.37 cm
Operating mode	TE_{01}
Operating cyclotron mode(s)	1
Beam voltage (V_b)	400 kV
Beam current (I_b)	2 kA
Guiding center position	$0.48 r_w$
Electron velocity ratio α (v_\perp/v_z)	0.7
Magnetic field (B_0)	3.7 kG
System length (L)	20 cm

Figure 1a displays the dispersion relations of the TE_{01} mode and beam cyclotron lines. The intersection point "A" is the desired backward wave oscillation. Using a cold and zero spatial spread beam, the beam annular width is only twice the beam Larmor radius. The beam plasma frequency (ω_b) can be evaluated and is about 0.524 of ω_c (waveguide cutoff frequency). Figure 1b shows the time evolution of output power determined from simulations. Without taking into account the effects of space charge field, the saturation efficiency is about 2%. Under the influence of the space charge field arising from the neutralized beam, the output power reduces slightly while the growth rate remains relatively unchanged. This is because in a gyrotron, the azimuthal phase bunching dominates over spatial bunchings. The AC space charge field plays a minor role. Figure 2 plots the spatial distribution of the beam electrostatic potential and electric fields. Outside the beam region, the field quantity does decay exponentially. The experimental result from Phillip's Laboratory indicates that the efficiency is much better (almost 10 times) if the TE_{21} mode is the operating mode. In order to simulate this results, a three dimensional electrostatic code is required. We intend to develop such a code by including a finite number of azimuthal modes. We are also working on electrostatic codes to simulate plasma-filled backward wave oscillators and helix traveling wave amplifiers. Both devices require periodic waveguide wall to slow down the electromagnetic wave propagation. We will also investigate the effects of a non-neutralized beam on the performance of gyro backward wave oscillators.

References

1. B. Goplen, L. Ludeking, D. Smithe, and G. Warren, Computer Physics Communication, 87, 54(1995).
2. Y. Y. Lau and D. Cherin, Phys. Fluids B, 4, 3473(1992).
3. J. D. Jackson, "Classical Electrodynamics," Chapter 6, (Wiley, 1975).
4. J. M. Dawson and A. T. Lin, "Particle Simulations," Handbook on Plasma Physics, Vol. II, Basic Plasma Physics. A. A. Galeev and R. N. Sudan, Eds., (Elsevier Science Pub., Amsterdam) Chapter 7, p. 555 (1984).
5. T. H. Kho and A. T. Lin, Nuclear Instruments and Methods in Phys. Research, A296, 8642(1990).
6. C. DeBoor, SIAM J. Numer. Anal., 14, 441(1977).
7. C. DeBoor and B. Swartz, SIAM J. Numer. Anal., 10, 582(1973).
8. A. T. Lin and Chih-Chien Lin, Physics of Fluids B5, 2314(1993).
9. T. A. Spencer, C. E. Davis, K. J. Hendricks, F. J. Agee, and R. M. Gilgenbach, IEEE Trans. on Plasma Science, 24, 630(1996).

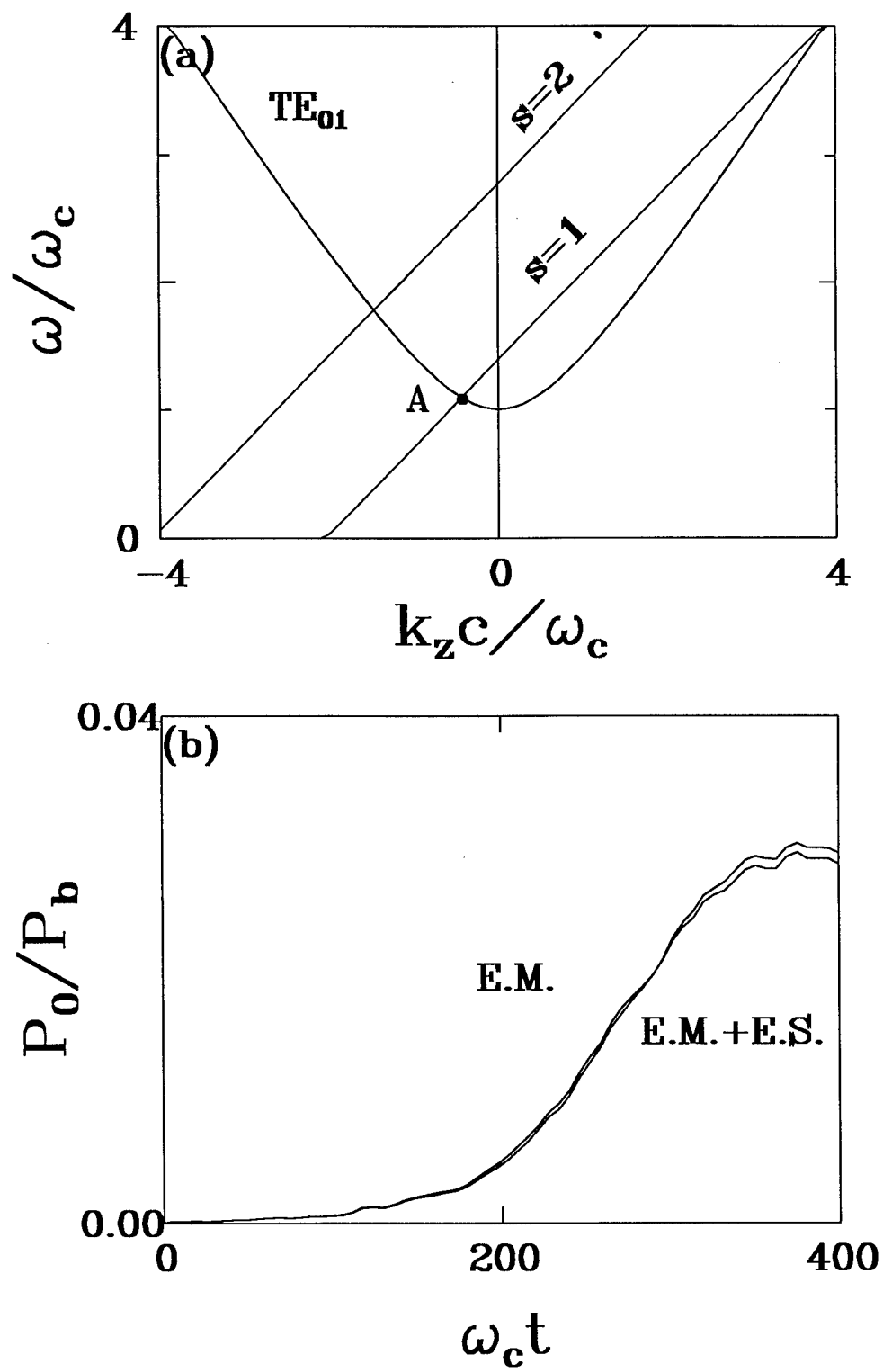


Figure 1 Gyro backward wave oscillation, (a) dispersion curves, and (b) time evolution of output wave power.

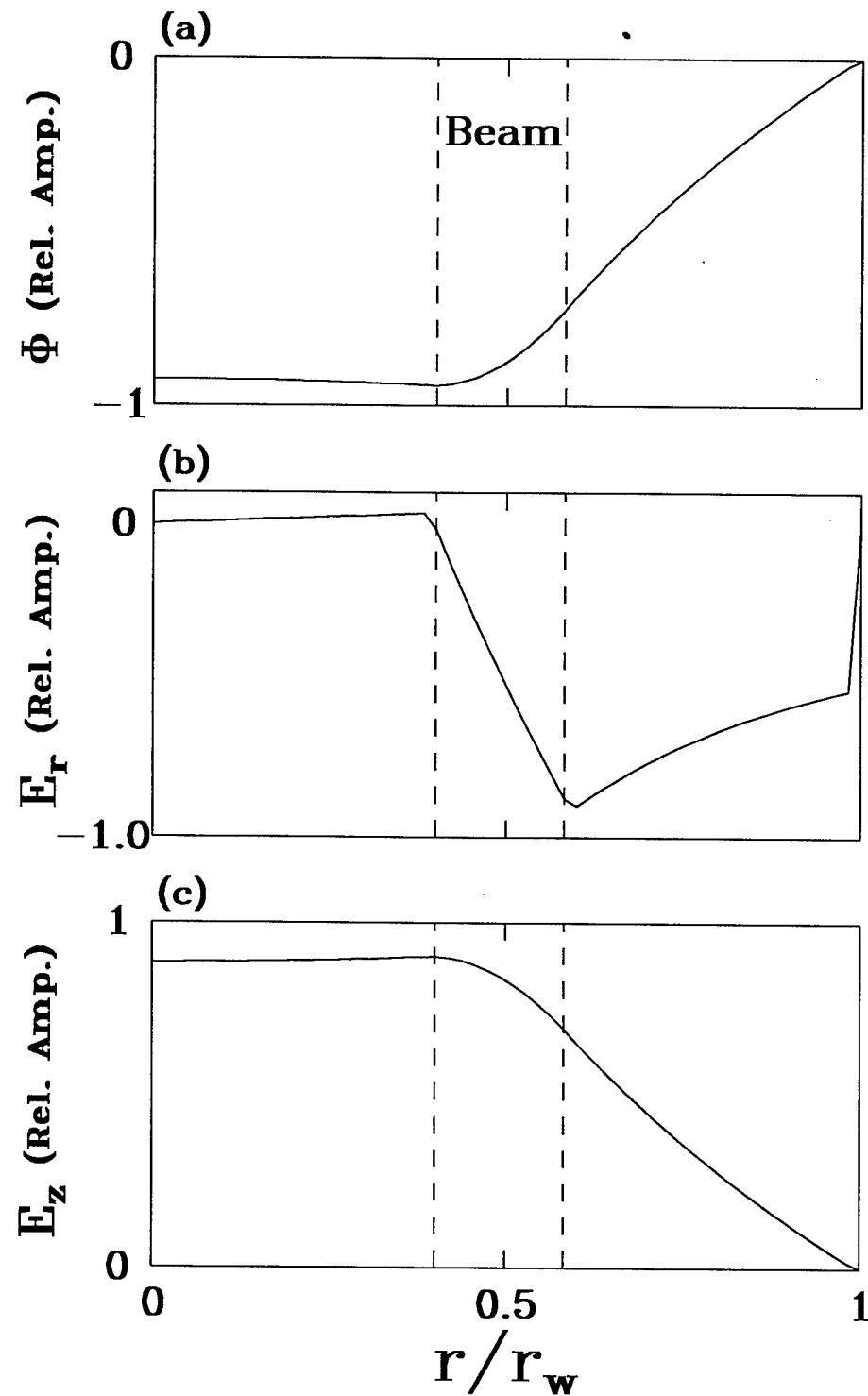


Figure 2 Transverse spatial distribution of electrostatic field ($k=1$), (a) potential, (b) radial electric field (E_r), and (c) longitudinal electric field (E_z).